Theoretical Ecology (2025) 18:6
https://doi.org/10.1007/s12080-024-00598-0

RESEARCH

Post-disturbance recovery dynamics of connected coral subpopulations

Walter I. Torres[1,6] · Daniel M. Holstein[2] · Hollie M. Putnam[3] · Peter J. Edmunds[4] · Jonathan B. Puritz[3] · Robert J. Toonen[5] · James L. Hench[6]

Received: 29 April 2024 / Accepted: 13 November 2024

Abstract

Coral reefs are patchy and connected ecosystems that experience heterogenous environmental conditions, disturbances, and coral population recovery patterns. Connectivity and population growth rates between reef patches can vary at local to subregional (1–100 km) scales, but current coral population models do not bridge the spatial gap between metapopulation-scale (i.e., 100–1000 km) and local population (patch-scale) dynamics (1–10 km). Here, we formulate a density-dependent logistic multi-population dynamics model for reef-building corals that includes the capacity for coral recruitment supported by larvae from autochthonous, local, and allochthonous sources. Model behavior is examined across an idealized parameter range, including limiting cases. It is then applied, with parameters derived from long-term field data sets, to hindcast and interpret the mechanisms driving the coral population recovery observed following a major disturbance. The data represent subpopulations on the fore reef and back reef habitats in Moorea, French Polynesia, that experienced a rapid increase in coral cover following large disturbances from crown-of-thorns sea star outbreak and cyclone in 2010. Analyses of the population model behavior suggest that the observed coral recovery from 2010 to 2019 on the fore reef of Moorea can be explained by an initial immigration of coral larvae from a metapopulation coupled with strong intrinsic growth. This result highlights the importance of population connectivity at scales larger than the spatial scale of disturbances, as well as local conditions conducive to post-settlement success and recovery.

Keywords Coral reefs · Population modeling · Resilience · Recovery

Introduction

Coral reefs are patchy ecosystems separated over local-to-subregional scales (1–100 km) that vary in environmental conditions and benthic community structure (Aronson and Precht 1995). Gene flow between coral populations is dependent on the transport of pelagic larvae over scales varying from centimeters to 1000 s of kilometers (Scheltema 1986). For a coral subpopulation, larvae supporting local growth could originate from many sources, and larvae produced locally may disperse to a wide variety of destinations. The persistence of coral reef patches is related both to local population growth and maintenance and to the recruitment subsidy supported by connected subpopulations (Hastings and Botsford 2006). A subpopulation might, at times, be self-sustaining, while at other times rely on larval subsidy from other subpopulations (i.e., from allochthonous sources) (Figueira 2009); most subpopulations would be expected to experience recruitment of larvae from a mix of these two

✉ Walter I. Torres
wtorres@uw.edu

1 Applied Physics Laboratory, University of Washington, Seattle, WA, USA

2 Department of Oceanography and Coastal Sciences, Louisiana State University, Baton Rouge, LA, USA

3 Department of Biological Sciences, University of Rhode Island, South Kingstown, RI, USA

4 Department of Biology, California State University Northridge, Northridge, CA, USA

5 Hawai'i Institute of Marine Biology, University of Hawai'i at Mānoa, Honolulu, HI, USA

6 Nicholas School of the Environment, Duke University, Beaufort, NC, USA

Published online: 30 December 2024

sources. Understanding population dynamics within a given subpopulation, therefore, requires examining the varying scales and relative importance of larval transport, recruitment, and local population growth. The need for such understanding is particularly acute for coral reefs that face habitat fragmentation through anthropogenic degradation (Hoegh-Guldberg et al. 2011), which is expected to limit migration within, and resilience of, networks of populations connected through larval migration (Darling and Côté 2018).

Metapopulation models provide a tool to understand the role of larval migration in population persistence. These models often assume homogenous within-patch (i.e., local) demographics (Hastings and Botsford 2006; Garavelli et al. 2018) or ignore them completely (Hanski and Ovaskainen 2000) and assume local equilibrium. Large declines in the size of coral populations are a relatively recent phenomenon (Dietzel et al. 2021), and metapopulation models that explicitly parameterize coral death, recruitment, and growth may be useful in identifying the processes driving changes in coral population sizes in complex seascapes (Holstein et al. 2022). The ratio of coral recruits originating from the settlement of local versus allochthonous larvae is likely to influence the rate and extent of local coral population growth following large declines in abundance. Many disturbances affecting coral population sizes act in a patchy fashion at a local scale (< 20 km) (Syms et al. 2000; Osborne et al. 2011), and among-patch variability of post-disturbance trends in coral abundance has been observed (Kayal et al. 2018).

The population dynamics of tropical scleractinians most commonly are described with coarse resolution through descriptions of overall coral cover (Hughes 1994) and less often with genus or species resolution (Reverter et al. 2022). Demographic models that capture vital rates (e.g., birth and death rates, intrinsic rates of population growth) remain relatively rare and have been codified by matrix models (Hughes 1984) and Integral Projection Models (IPMs; Merow et al. 2014), yet applications of such approaches are scant. Ordinary differential equation (ODEs) models provide alternative means to describe coral population dynamics, but most applications have focused on competitive dynamics among corals, macroalgae, and herbivorous fishes (e.g., Mumby et al. 2005) rather than relating intraspecies connectivity to coral population growth.

Here, we address the role of coral larvae originating from source colonies at three different spatial scales mediating coral population growth following large and spatially structured declines in coral abundance. These scales are defined as (a) allochthonous, originating from sources 10–1000 km away, (b) local originating from sources 100 m–10 km away, and (c) autochthonous, originating from sources 1–100 m away (i.e., self-seeding within discrete coral patches). We rationalized that the spatial pattern and temporal pace of coral population recovery should be influenced by the relative rates of population growth supported by larvae from these different sources. Further, we suggest it will remain highly challenging to understand the ecological resilience of a coral reef without understanding the relative contributions of these separate and dynamic processes to the maintenance of coral populations.

We employ a conceptual and numerical modeling approach in which coral populations grow logistically while influenced by asexual growth and sexual recruitment supported by larvae originating from three scales of source colonies. For a coral patch, population growth could be due to (1) asexual growth of extant and relict coral colonies to produce new polyps, (2) sexual recruitment supported by larvae originating within the patch, (3) sexual recruitment supported by larvae originating from nearby isolated coral patches 100–10 km away, and (4) sexual recruitment supported by larvae originating from corals > 10 km away (Fig. 1). Because coral reefs often form continuous structures consisting of heterogeneous communities scattered among multiple habitats, we have coupled models of two adjacent reefs, each containing forereef and backreef habitats in which coral subpopulations are found.

After formalizing our numerical model, we apply it to a well-studied coral reef in Moorea, French Polynesia. The advantage of focusing on the reefs of Moorea is that there are decades of data describing rates of coral growth and recruitment for this system. Importantly, the fore reef has gone through a cycle of near-complete local death in 2010,

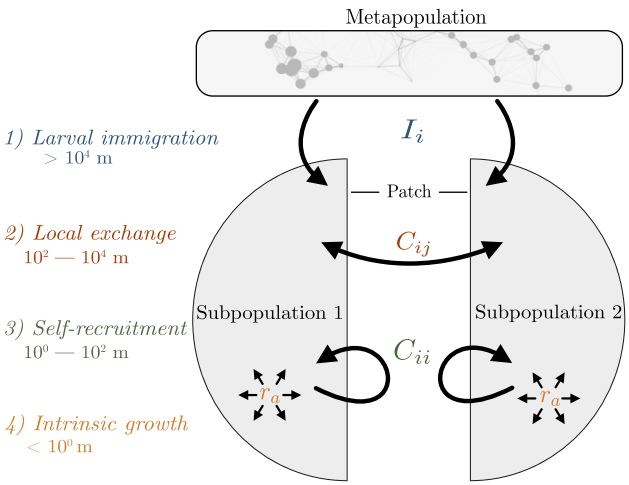

Fig. 1 Conceptual diagram illustrating subpopulations and the processes accounted for in the population model developed here. Coral population change can occur through (1) immigration to reef patches from the metapopulation (allochthonous recruitment); (2) local exchange between reef patches; (3) reproduction via sexual self-recruitment (autochthonous); and (4) reproduction via asexual intrinsic growth. The exchange matrix C_{ij} represents the probability of recruitment by a given planula with (source, sink) population (i, j)

population recovery over nine years to 2019 (Edmunds et al. 2018), and a new cycle of population decline commencing in 2019 (Burgess et al. 2021). These dynamics have not been spatially uniform with this outcome attributed to variation in coral recruitment and post-settlement success (Holbrook et al. 2018; Edmunds et al. 2024). The highest rate of coral recruitment and most robust coral population recovery was detected on the north shore (Holbrook et al. 2018). However, the mechanisms facilitating this outcome are not fully understood, and there is little information on the source(s) of the coral larvae that supported this population growth. Herein, we develop and test this multi-scale population model, which is generally applicable to connected subpopulations of sessile marine organism exhibiting a biphasic life cycle with pelagic larvae (e.g., most bryozoans, scleractinians, octocorals, and ascidians).

Materials and methods

Model formulation

Here, we develop a mathematical population model of ecologically connected, spatially heterogeneous coral subpopulations. We represent population change as a system of modified compartmental logistic growth equations (Verhulst 1845; Pulliam and Danielson 1991). First, we consider a single coral subpopulation, where dP/dt is the change in population defined as the total number of individuals. Change in population size can occur through asexual proliferation and mortality (r_a), sexual reproduction through recruitment (r_e), and net immigration (I). Fecundity (f), larval maturation probability (ζ), larval dispersal (γ), recruitment probability (β), and recruit size class (σ) all influence the magnitude of r_e. Immigration (I) describes recruitment sourced extrinsically from subpopulation(s) as non-negative and constant through time, assuming that there is a background stable metapopulation with persistent connectivity to an individual population (Fig. 1). Growth and mortality are assumed to be density-dependent; an assumption we make for coral reefs where there is limited available substratum for growth and a combination of local predation, disease, and competition dynamics determine the carrying capacity (Vermeij and Sandin 2008). All model parameters (besides P) are assumed to be time-invariant, so the single population model can be formulated as

$$\begin{aligned} \frac{dP}{dt} &= [PR + I]\left(1 - \frac{P}{K}\right) \\ R &= r_a + r_e \\ r_e &= f\zeta\gamma\beta\sigma \end{aligned} \tag{1}$$

A more general form of Eq. 1 can be written to describe multiple coupled populations, where model variables (P, K, I, f, ζ, σ) are $N\times 1$ vectors and (β, γ) are $N\times N$ matrices, where N is the number of connected populations considered. A matrix–vector approach permits the parameterization of asymmetric fitness and fertility properties (f, ζ, β) of individuals from different populations, as well as differential individual exchange (γ) between and within subpopulations. Here, the row index (i) indicates the donor population, and column index (j) indicates the receiver population. For example, the larval dispersal term γ_{ij} indicates which fraction of larvae produced by P_i are transported to P_j as possible recruits, hence, $\sum_{j=1}^{n}\gamma_{ij}$ and $\|\gamma\|_{\max}\leq 1$. Of those, β is the fraction that recruits the receiver population and matures to a certain size class (σ). An exchange matrix (C) is used to represent the combined probability of successful recruitment and maturation of larvae to a population, where $C_{ij}=f_{ij}\odot\zeta_{ij}\odot\gamma_{ij}\odot\beta_{ij}\odot\sigma_{ij}$, and ($\odot$) is the Hadamard product (element by element multiplication).

$$\frac{dP_j}{dt} = \left[\underbrace{P_j r_j}_{\text{asexual growth}} + \underbrace{\sigma f\zeta(\gamma\odot\beta)^{\mathrm{T}}_{jk}P_k}_{\text{local and self-recruitment}} + \underbrace{I_j}_{\text{immigration}}\right]\underbrace{\left(1-\frac{P_j}{K_j}\right)}_{\text{density dependence}} \tag{2}$$

This formulation permits explicit parameterization of key physical and biological processes that control population change for a system of connected populations each with potentially unique characteristics.

We now use idealized applications of the model to explore the fundamental behavior of the coupled two-population system. First, we non-dimensionalize Eq. 1 using an intrinsic time scale ($\tau=Rt$) set by internal growth dynamics and self-recruitment, where the population is scaled by the carrying capacity ($P_j^*=P_j/K$) and immigration rates are scaled by the product of the immigration time scale (S) and the carrying capacity $I^*=I_j/(SK)$. If we consider a case where the two populations have identical growth rates ($r_1=r_2=1$), carrying capacities ($K_1=K_2=1$), and the exchange matrix is positive semi-definite ($C_{ij}=1$ for $i\neq j$ and $C_{ij}=0$ for $i=j$), then Eq. 2 reduces to a growth model for two non-dimensional populations ($P_i=P^*K$). For two populations with equal growth rates and initial conditions, it is expected that inter-population larval donation will occur on the same time scale as internal growth, so we claim $C/R=1$, further simplifying the equations.

$$\begin{aligned} \frac{dP_1^*}{d\tau} &= \left(P_1^* + P_2^* + \frac{I^*}{\Gamma}\right)\left(1-P_1^*\right) \\ \frac{dP_2^*}{d\tau} &= \left(P_2^* + P_1^* + \frac{I^*}{\Gamma}\right)\left(1-P_2^*\right) \end{aligned} \tag{3}$$

The coefficient $\Gamma=R/S=C/S$ can thus be considered the non-dimensional parameter that governs the relative importance of exponential local growth dynamics versus a linear external recruitment source. When Γ is negative, the equations

become coupled logistic growth with a constant in time mortality/harvesting or emigration term, a problem considered in introductory differential equations textbooks and in marine resources economics (e.g., Husniah and Supriatna 2014; Moeller and Neubert 2015). Sessile organisms like reef corals cannot emigrate, so Γ represents the net growth by asexual processes and mortality by predation, harvesting, or disease.

We now consider population trajectories for limiting cases where immigration or intrinsic growth is dominant, as well as an intermediate case where both processes are important ($\Gamma = 10$) (Fig. 2). Small Γ regimes are characteristic of linear growth until the population approaches carrying capacity, while large Γ regimes are characteristic of classical logistic-type growth curves. Where both processes are relevant for population growth, the shape of the growth curve is somewhere between those end members, with the presence of immigration facilitating a more rapid recovery from low population initial conditions. An interesting demographic consequence of immigration initiating a more rapid recovery is that the allochthonous sourced population (i.e., immigrants) are the ones that benefit from a locally favorable growth curve and end up comprising the majority of the population at carrying capacity. The significance of this demographic phenomenon should be proportional to the non-dimensional quantity $\Gamma P_0/K$. As $\Gamma P_0/K$ increases, so would the relative dominance of the local growth of an initial autochthonous population over the intrinsic or extrinsic growth of the allochthonous population. In this example, $\Gamma P_0/K = 0.1$ which is consistent with the relative demographic dominance of the allochthonous population. In the case that one population is drastically larger than the other (not plotted) and is connected to the other via local exchange,

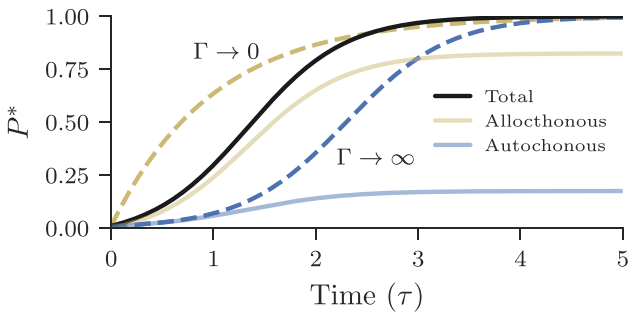

Fig. 2 Nondimensional population recovery trajectories according to Eq. 3. Both subpopulations (P_1, P_2) are assumed identical so only one population trajectory is shown. The dashed lines are population trajectories for limiting cases where immigration (yellow) and intrinsic growth (blue) dominate. The solid lines show population recovery trajectories for an intermediate case of $\Gamma = 10$. The black line is the total population growth — the sum of the allochthonous (yellow) and autochthonously sourced (blue) contributions. The initial populations were set to $P_0^* = [0.01, 0, 01]$ and assumed to be entirely autochthonous

the trajectory of the recovering population resembles that of the $\Gamma \to 0$ case. In a system unaffected by allochthonous immigration, the potential for subpopulations to self-seed or rescue another from disturbances could be quantified by the diagonal dominance of the exchange matrix (C). One such condition, from the Levy-Desplanques theorem, is $|C_{ii}| > \sum_{j \neq i} |C_{ij}|$.

Application of model to a coral reef system

The model developed above is now applied to understand coral community dynamics that have been observed on the coral reefs of Moorea, French Polynesia. Here, the coral community on the fore reef is separated from the coral community in the back reef by a reef crest, over which wave-driven currents determine the extent to which coral propagules exchange between habitats (Hench et al. 2008; Monismith et al. 2013; Lindhart 2022). These reefs are mostly populated by corals that engage in mass spawning to generate pelagic larvae with larval durations of days-weeks (Carroll et al. 2006; Baird et al. 2009) and periodically are impacted by disturbances (e.g., Crown of Thorn sea stars [COTS], cyclones, and bleaching) having differential impacts in back reef and fore reef habitats (Edmunds et al. 2010). Although analyses of the population genetics of corals on the reefs of Moorea are limited in scope, it is possible that larvae of the dominant coral, *Pocillopora* spp. (spawning species representing a suite of cryptic species) (Burgess et al. 2021; Johnston et al. 2022), that seed the reefs of Moorea could be sourced from both local (i.e., Moorea) or more distant locations (i.e., Tahiti, 16 km to the east). From 2005 to 2018, these reefs have demonstrated a transition in which the fore reef community has quickly changed from 38% cover in 2005 to near zero cover in 2010, with recovery to reach a mean coral cover at 10 m depth of 81% by 2018. The coral community in the back reef has changed in dissimilar ways over the same period, generally undergoing declining in coral cover and increasing in cover of macroalgae. One recent cycle of coral death and subsequent recovery was driven by a large outbreak of COTS that consumed corals on the fore reef from ca. 2005 to 2010, and subsequently, most of the dead-in-place coral skeletons were removed by Cyclone Oli. Afterward, the forereef coral community in 2011 experienced a rapid recovery (Holbrook et al. 2018). While this recovery has been dominated by pocilloporid corals, other coral genera also have been recruited, so the multivariate coral community structure in 2018 was similar to that recorded in 2005 (Adjeroud et al. 2017). The present modeling approach draws on empirical data from these reefs recorded as part of a long-term ecological time series (LTER) effort based in Moorea, French Polynesia, and focuses on the events taking place on the north shore between 2010 and 2018.

We partition Moorea's pocilloporid populations into fore reef and back reef habitats, which are permitted to have different demographic properties (as informed by field observations) and are connected through ocean circulation-driven larval dispersal. We assume σ and f are representative of pocilloporid reproduction at all locations, so can be written as a system of two coupled nonlinear ODEs.

$$\begin{aligned}\frac{dP_b}{dt} &= \left(P_b(r_b + \sigma f \zeta(\gamma\beta)_{b\to b}) + \sigma f \zeta(\gamma\beta)_{f\to b}P_f + I_b\right)\left(1 - \frac{P_b}{K_b}\right)\\ \frac{dP_f}{dt} &= \left(P_b(r_f + \sigma f \zeta(\gamma\beta))_{f\to f}) + \sigma f \zeta(\gamma\beta)_{b\to f}P_b + I_f\right)\left(1 - \frac{P_f}{K_f}\right)\end{aligned} \tag{4}$$

where the subscripts b and f indicate fore reef and back reef coral subpopulations respectively. We cast the model in terms of the number of polyps instead of the number of colonies, so that we can consider the relationship between fecundity, recruitment, individuals (i.e., polyps), and population growth in the same units. Fecundity (egg/polyp) is assumed constant, which translates to a positive relationship proportional to colony size (Hall and Hughes 1996; Alvarez-Noriega et al. 2016; Holstein et al. 2022). It is assumed that half of all eggs are fertilized and produce viable planula ($\zeta = 0.5$). Data to constrain larval fertilization and maturation are unavailable for our study site, so $\zeta = 0.5$ is based on prior work in other broadcast spawning coral *Montipora* (Padilla-Gamiño and Gates 2012). Carrying capacity and growth rate are expressed in terms of two-dimensional planar surface. Together, this allows our model to be formulated in general terms to consider the dynamics of multiple populations of sessile, colonial organisms that are connected through larval transport. This formulation allows for potentially asymmetric transfer from one subpopulation to another. The advantage of this approach is that a single model allows both individual asexual growth and recruitment-driven growth to be considered simultaneously, without needing to model life stage transitions.

This system of ODEs (Eq. 4) was numerically integrated using Scipy's *odeint* function (Virtanen et al. 2020) and fit to Monte-Carlo simulations of observational data ($n = 50$) within uncertainty bounds derived from observations to examine the range of possible recovery outcomes. Values of (f, σ) were fixed based upon prior studies (Tricas 1989), and K was computed based on the available substratum and area (Appendix). Thus, the degrees of freedom in the model lie in the asexual growth rate (r_a), immigration rate (I), and the product of transport and recruitment fraction ($\gamma \odot \beta$). These quantities, although difficult to measure, must reproduce the observed population growth trajectory. The coral population can only increase in size through asexual and sexual processes, and both can be estimated with the proposed model. The parameters (R, C, I), where $C_{ij} = \sigma f \zeta\gamma_{ij}\beta_{ij}$, were fitted to empirical data using the differential evolution global optimization method (Virtanen et al. 2020) that minimizes an objective functional (J), a weighted mean coefficient of determination of the modeled versus the observed coral cover at the forereef and backreef. The weighting was used to ensure the trajectories of both forereef and backreef populations were well-represented, while biasing in favor of representing forereef populations which showed orders of magnitude more growth.

$$J = A\frac{\sum_{i=1}^{n}\left[P_b(t_i) - \widehat{P_b}(t_i)\right]^2}{\sum_{i=1}^{n}\left[P_b(t_i) - \overline{P_b}\right]^2} + B\frac{\sum_{i=1}^{n}\left[P_f(t_i) - \widehat{P}_f(t_i)\right]^2}{\sum_{i=1}^{n}\left[P_f(t_i) - \overline{p}_f\right]^2} \tag{5}$$

where $A = 0.1$ and $B = 0.9$ were chosen and $\widehat{P}$ are the modeled population values. Model fits with $1 - J < 0.95$ were excluded from the analysis.

Field observations of the density of small colonies of *Pocillopora* spp. (Fig. 5) were used to establish an upper bound on self-recruitment and infer a lower bound on asexual growth. For each model fit, recruitment flux (ρ) was assumed to be the upper 95% confidence interval bound for ρ as derived from bootstrapping. This limit can be used with the total growth rate (a combination of asexual and self-recruitment: $R_i = r_i + C_{ii}$) to solve for the self-recruitment terms of C_{ij} once R_i has been inferred from the model fit.

$$\left(C_{ij}P_i(t) + I_i\right)\left(1 - \frac{P_i(t)}{K_i}\right) < \rho_i(t) \tag{6}$$

Equation (6) was evaluated at $t = 2014$ for which the density of small *Pocillopora* spp. previously was estimated (Tsounis and Edmunds 2016). A planula conservation constraint should also be used in general applications of the proposed model ($0 \le \Sigma_k \gamma_{jk} \le 1$); that is, there cannot be more recruits sourced from local populations than the total number of larvae available. In our application, however, bounding recruitment from field observations was sufficiently strict (Eq. 6), as the total possible recruitment was expectedly much lower than the theoretical maximum. The fraction of recruits that successfully mature into small colonies should also be constrained ($\beta \le 1$), but it cannot be constrained independently from the transport fraction ($\gamma \le 1$), which is also not known. In future work, hydrodynamic modeling could be used to estimate γ (e.g., Mitarai et al. 2009). Before proceeding, it is important to point out that in this model, self-recruitment (on-diagonal terms of the C_{ij} matrix) behaves identically to the asexual growth term; both are nonlinear exponential growth terms. Thus, fitting the model to data produces an estimate of the total growth rate (R).

Results

Model hindcasts recovered observed population trajectories for *Pocillopora* spp. on two forereef sites (LTER 1 and LTER 2) with high fidelity ($r^2 > 0.95$; Fig. 3a, b). The shape of the fore reef growth curves indicates that logistically behaving internal dynamics (i.e., self/local recruitment and/or asexual growth) dominated the recovery at each site. This prediction implies that a majority of population growth was supported by allochthonous sources by up to a factor of two (Fig. 3a, b). Parameter estimates of coral population growth rate and larval immigration correspond to $\Gamma P_0/K \approx 0.1$, resembling the intermediate idealized case (Fig. 2) and consistent with the demographic dominance of allochthonous sourced growth. Asexual polyp growth contributed more to the total population growth than self-recruitment at both forereef sites, while local exchange between forereef and backreef sites was negligible.

Due to sparse observations and the absence of growth, modeled *Pocillopora* spp. population dynamics in the back reef at both sites (Fig. 4a, b) were ill-constrained. However, a steady decline in coral cover since 2011 is consistent with other observations of an increasingly macroalgal-dominant regime (Han et al. 2016). The coupling between the back reef and the fore reef through the exchange recruitment term was negligible at both sites, but this does not preclude the existence of local exchange processes with other unmodeled regions of the reef. The upper range of modeled $(\gamma\beta)_{ff}$ values are of order 10^{-2}; therefore, $0.01 < (\gamma_{ff}, \beta_{ff}) < 1$, indicating high self-retention and successful self-recruitment.

Discussion and conclusions

Our model has isolated some of the mechanisms that can mediate coral population recovery after disturbance on the north shore of Moorea. By partitioning population growth into intrinsic (asexual growth and self-recruitment) and extrinsic (immigration) contributions, we have transitioned empirical observations of coral recruitment and population growth into assessments of the relative contributions of these intrinsic and extrinsic factors to recovery after disturbance. We have shown that in the absence of substantial immigration, recovery from extreme mortality will appear logistic. Contributions to recruitment by nearby populations (within the reef) can support population recovery; however, unlike immigration, which in our model is constant and non-zero, this intra-reef exchange will scale with subpopulation size.

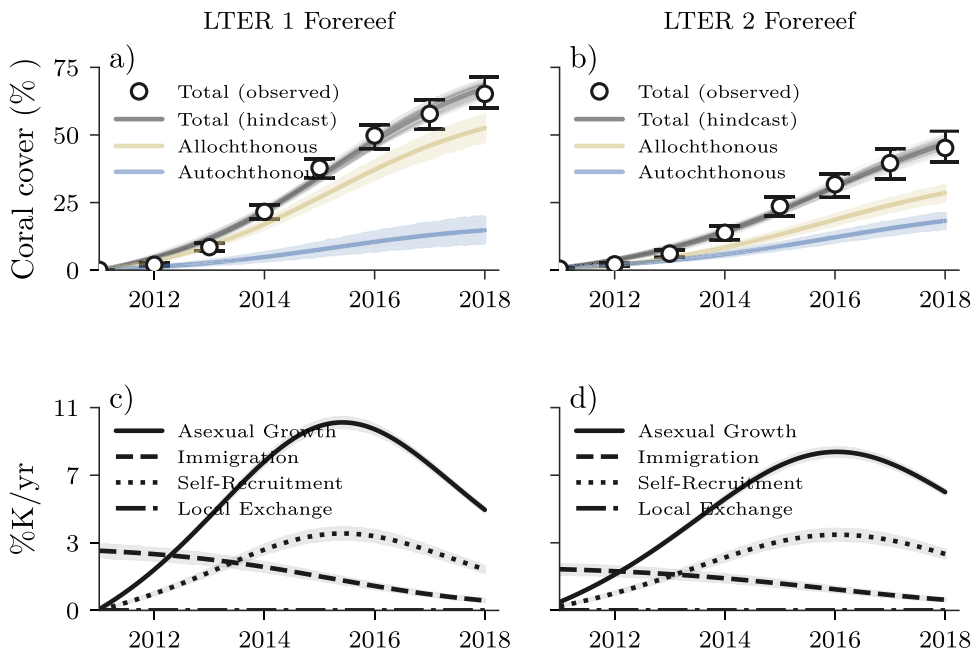

Fig. 3 **a**, **b** Model hindcasts of population trajectories for *Pocillopora* spp. on the forereef at sites LTER1 and LTER2 on the north shore of Moorea showing the total population growth (black) from autochthonous (blue) and allochthonous (yellow) sources. Ninety-five percent confidence intervals are shaded around the autochthonous and allochthonous population trajectories based on 100 different successful model fits. Every hindcast of the total population is displayed as a thin black line with opacity while the mean is a thicker gray line. Observed coral cover measurements and 95% uncertainty bounds are shown with the scatter points and error bars. **c**, **d** Components contributing to the change in population growth (*dP/dt*) decomposed into the terms in Eq. 4. Term magnitudes are expressed as percent of the populations' carrying capacity per year

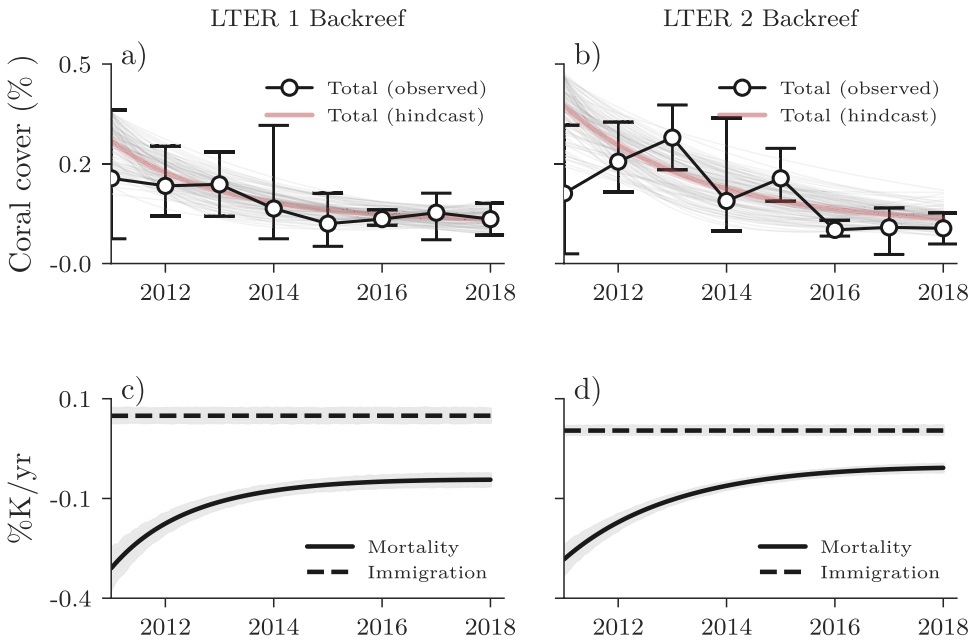

Fig. 4 **a**, **b** Model hindcasts of population trajectories for *Pocillopora* spp. on the backreef at sites LTER1 and LTER2 on the north shore of Moorea. Every hindcast of the total population is displayed as a thin black line with opacity while the mean is a thicker red line. Observed coral cover measurements and 95% uncertainty bounds are shown with the scatter points and error bars. **c**, **d** Components contributing to the change in population growth (*dP/dt*) decomposed into the terms in Eq. 4. Term magnitudes are expressed as percent of the populations' carrying capacity per year. Only mortality and immigration are shown here because the local exchange terms were negligible

The logistic shape of recovery trajectories for *Pocillopora* spp. on Moorea's fore reef is consistent with *Pocillopora* spp. recovery on reefs elsewhere in French Polynesia after several strong cyclones impacted the region during 1997–1998 (Vercelloni et al. 2019). The similarity between population response curves implies similar recovery mechanisms and limitations, i.e., high growth rate, density-dependence, and connectivity to populations outside the scales of disturbance. Cyclones and crown-of-thorns sea star outbreaks do not uniformly impact coral populations on reefs in French Polynesia (Adjeroud et al. 2005), so it is possible that mildly disturbed reefs can contribute larvae to strongly disturbed ones, defined as immigration in the model developed here. A range of values for intrinsic growth rate and larval immigration fit the modified logistic population model to our empirical data ($r^2 > 0.95$). On the reef, these parameters may vary in space and time. Thus, throughout the coral population recovery on Moorea's north shore (i.e., 2011–2018), immigration and intrinsic growth may have fluctuated, which may be captured within the derived parameter confidence intervals. We have lower confidence in parameterizations for the back reef because coral population recovery was not empirically observed. Disturbance by other mechanisms (nutrient loading, predation, etc.) may be ongoing or the backreef may have entered an alternative stable state with a reduced coral carrying capacity (Schmitt et al. 2019).

The model results indicate that the recovery of Moorea's north-shore coral communities is likely to be a product of the confluence of local and remote conditions. Initial immigration of *Pocillopora* spp. larvae from allochthonous sources, which may have avoided the effects of COTS and Cyclone Oli, experienced post-settlement growth and began self-seeding. These allochthonous-sourced *Pocillopora* spp. recruits may have originated from patches of undisturbed coral reef habitat (Holstein et al. 2015), or from different islands in French Polynesia (Magalon et al. 2005); the likelihood of these two possibilities could be tested using population genomic techniques. After 2013, model results suggest asexual polyp growth dominated recovery, and recruitment from locally produced larvae surpassed the immigration subsidy. This is consistent with observations elsewhere on the north shore of Moorea, where coral recovery has been detected even with low coral recruitment, implying high recruit survivorship (Adjeroud et al. 2017). That an initial influx of sustained allochthonous recruitment is required to initiate the population recovery trajectories (Fig. 3c, d) is consistent with other population modeling work conducted on Moorea (Kaya et al. 2018). Hindcasted estimates of the potential role of self-recruitment are quite large, which indicates that other reefs on Moorea with similar recovery trajectories, unaccounted for in this model, may have contributed larvae to the fore reef of Moorea. The divergence of coral population trajectories between the fore reef and the back reef highlights that conditions on the fore reef were conducive to the asexual proliferation of polyps (i.e., colony growth) that originated from recently settled larvae. On the back reef, intrinsic growth was balanced, or outweighed, by mortality, making a coral population recovery difficult despite larval subsidy from a recovered coral community on the fore reef. The relative dominance of self-recruitment to subpopulation exchange implies that the exchange matrix (C) is diagonally dominant. As the habitats are hydrodynamically connected (Hench et al. 2008), it is more likely

that back reef conditions are not conducive to larval settlement and recruitment, rather than not experiencing a larval flux from the fore reef. While the local exchange of larvae between the back reef and fore reef coral subpopulation may play an important role in population dynamics, it likely did not on Moorea over the study period.

The interplay of immigration and self-recruitment affects the shape of the recovery trajectory for coral cover (Fig. 2). If disturbance of the fore reef prior to 2011 had been less extreme, locally produced *Pocillopora* spp. larvae and asexual colony growth would probably have been the dominant sources of initial population recovery, and a subsidy from immigration would not have been necessary. This has implications for the genetic relationships among corals within a reef and supports the assertion that the frequency and magnitude of disturbances could affect local coral adaptation and the exchange of advantageous genes (Quigley et al. 2019). Additionally, there are implications for coral reef management. Here, our model was used to hindcast the population growth dynamics of coral subpopulations, but in theory, it could be used prognostically to explore the effect of coral reef management interventions. Interplay between the connectedness of subpopulations, metapopulation larval input, and intrinsic growth rates on a given reef may favor certain management strategies to bolster resilience. For instance, a highly disturbed reef may be resilient to collapse if it is well-connected to populations beyond the spatial scale of the disturbance. Enhancing connectivity to the metapopulation or asynchronously disturbed local subpopulations would improve resilience against disturbances at their respective scales. A weakly disturbed reef, however, may not require intervention or restoration beyond the maintenance of environmental conditions that are conducive to coral growth. Operationally, the predicted management intervention effect on demographic and connectivity properties could be used to compare between scenarios, aiding decision-making.

Future modeling work might benefit from examining the continuous demographic structure of corals post-disturbance, which could reveal the relative role of recruitment versus asexual growth (Artzy-Randrup et al. 2007). The effect of age-dependent growth rate and recruitment will have markedly different demographic signatures (Hughes 1984). Purely asexual growth-dependent population recovery from near extirpation would result in coral size classes that were uniformly represented by colonies, while purely recruitment-driven recovery would result in a demographic structure with wider size class variance in colony abundance. Thus, fitting field observations of the abundance of coral colonies by size class to demographic population models may be able to discern between the contributions of population growth from sexual reproduction versus recruitment. Demographic parameters such as mortality and fecundity also vary in time and with senescence (Rinkevich and Loya 1986), potentially influencing population structure. Future modeling efforts may apply the modeling framework developed here to consider more nuanced processes. For instance, allowing for time-dependent model parameters governed by shorter time-scale processes (predator–prey, competition, circulation modeling to infer larval connectivity, etc.) may provide more realistic hindcasts and predictions.

Appendix. Data to support model parameterization

Demographic state variables informing the model were estimated for the fore reef (10 m depth) and back reef habitats at LTER1 and LTER2 for subsets of years between 2011 and 2018 as part of the Moorea Coral Reef Long-Term Ecological Research (MCR LTER) project (https://mcr.lternet.edu). Most of the state variables were expressed at a genus level (*Pocillopora* spp.), which reflects the capacity to identify these corals by morphology. Our objective was not to provide a definitive description of the coral populations at the sites and habitats, in part because this is impossible to accomplish for *Pocillopora* spp. This genus of corals is represented by a suite of sympatric cryptic species (Burgess et al. 2021; Johnston et al. 2022) that cannot be resolved by morphological features as utilized during in situ surveys and analyses of photoquadrats. Following Burgess et al. (2021) and Johnston et al. (2022), it is likely that we have parameterized our model with varying combinations of data from at least four species (*P. grandis*, *P. verrucosa*, *P. meandrina*, and *P. tahueniensis*) and two haplotypes; based on the distribution of the common brooding coral *P. acuta* in Moorea, it is unlikely that this coral is included in our empirical sampling. Further, our primary objective was to develop a mathematical model to evaluate the role of locally—versus distantly—sourced larvae in supporting recruitment to coral populations. We sought to parameterize this nascent model with ecologically relevant biological state variables and sought these values through a coarse-grain analysis of available empirical data, much of which often was collected for purposes other than for the present study. These state variables are likely to have low accuracy, improvement of which is a necessary goal of future research.

Abundance of *Pocillopora* spp. colonies

Estimates of the density (colonies 0.25 m^{-2}) of *Pocillopora* spp. colonies were informed through the abundance of colonies that were inferred to be adult (i.e., sexually mature, > 4 cm in diameter). For the fore reef, the abundance of *Pocillopora* spp. colonies was estimated from surveys of colonies operationally defined as *P. verrucosa* based on corallum morphology (after Veron 2000), and these were obtained from photoquadrats (0.5 × 0.5 m) recorded at fixed locations along a single

permanently marked transect (40 m in length) at LTER1 and LTER2 in 2010, 2014, and 2017. At each site, 38–40 photoquadrats were surveyed in 2010 and 2014, and 15 were surveyed in 2017.

For the back reef, the abundance of *Pocillopora* spp. was estimated from photoquadrats (0.5 × 0.5 m) and in situ surveys in 1 year. Photoquadrats were used to estimate colony abundances in 2010, and these were recorded around five focal bommies at each of LTER1 and LTER2 that support the MCR LTER benthic time series in this habitat. Around each bommie, five photoquadrats were recorded along 5 m transects along each cardinal axis ($n = 100$ photoquadrats site^{-1}), and these were used to estimate the abundance of adult colonies of *P. verrucosa* as described above. Colony abundances from photoquadrats were augmented with data from 2017, but these were obtained from a single bommie at each site ($n = 20$ photoquadrats site^{-1}). To estimate abundances in 2014, we used in situ surveys completed in January 2015 as part of another study (Tsounis and Edmunds 2016). These surveys focused on *Pocillopora* spp. colonies regardless of size and were completed at two haphazardly selected locations close to LTER1 and LTER2 (17.479281°S, − 149.844869°W and 17.475370°S, − 149.803317°W), where plots of known (but variable) size (1.4–25.8 m^2, $n = 38$) were surveyed.

Percentage cover of *Pocillopora* spp.

The percentage cover of *Pocillopora* spp. was obtained from MCR LTER photoquadrats (0.5 × 0.5 m) recorded in the fore reef (10 m depth) and back reef at LTER1 and LTER2 from 2011 to 2017. On the fore reef, 40 photoquadrats were recorded annually at fixed locations along a 40 m transect at each site, and they were analyzed for corals with genus resolution. Analysis was completed by manually annotating 200 randomly located dots on each image using CoralNET software (Beijbom et al. 2015), and here, the cover of *Pocillopora* spp. is reported. In the back reef, photoquadrats were recorded annually around five focal bommies at each site, with each bommie sampled with 5 photoquadrats (0.5 × 0.5 m) recorded at random locations along 5 m transects placed along cardinal axes on each bommie (20 photoquadrats bommie^{-1}). As part of the MCR LTER project, these photoquadrats are analyzed with 4% resolution by scoring the dominant functional group occupying benthic surfaces within 25 sub-squares of each photoquadrat, thus providing a measure of coral cover (pooled among taxa). To estimate the cover of *Pocillopora* spp., a subset of photoquadrats (for 2012, 2013, and 2016–2018) at both sites also were analyzed with coral genus resolution using CoralNET software as described above. These analyses were revealed at *Pocillopora* spp. amounted to a mean (± SE) of 1.5 ± 0.4% of the coral cover at LTER1, and 1.9 ± 0.9% at LTER2 (both, $n = 15$ bommie replicates). These values were used to estimate the cover of *Pocillopora* spp. in all other back reef cases where coral cover was determined.

Density of small colonies of *Pocillopora* spp.

Small coral colonies of *Pocillopora* spp. were defined as colonies ≤ 4 cm in diameter, and their density was estimated by several means. On the fore reef, densities of small *Pocillopora* spp. were recorded in situ during 2010, 2014, and 2017 using 0.5 m × 0.5 m quadrats positioned at the same spots along the permanently marked transects used for the MCR LTER time series photoquadrats (described above for coral cover) ($n = 40$ quadrats site^{-1} year^{-1}). In the backreef, densities of small *Pocillopora* were obtained from photoquadrats in 2010 and 2017, and from in situ counts estimated from various sources. For 2010, data are reported from LTER 1 and 2 backreef sites in January 2015 (used as an estimate of 2014 density). The photoquadrats used for this purpose are the same ones described above for coral cover, and here 100 photoquadrats (20 around each of five bommies) were screened at LTER 1 and LTER2 in 2010, and 20 were screened around one bommie at each site in 2017. All small colonies of *Pocillopora* spp. were counted to provide densities in units of colonies 0.25 m^{-2}. For 2014, densities of small colonies were determined in situ during January 2015, when plots of known (but variable) size (1.4–25.8 m^2, $n = 38$) were surveyed at sites close to LTER1 and LTER2 (described above); data were expressed as colonies m^{-2} (Fig. 5).

Because our model was based on a *Pocillopora* spp. replicate defined as a polyp, the abundances of small *Pocillopora* were converted to polyp abundances using an area-normalized polyp density of 66 polyps cm^{-2} (for *Pocillopora* spp. (Tricas 1989)) and an estimated area on small coral assuming they were all flat disks with a diameter of 2 cm. With this rationale, each small *Pocillopora* spp. contains 829 polyps (σ).

Growth rate of *Pocillopora* spp. colonies (r_a)

The growth rate of *Pocillopora* spp. colonies was quantified as the annual planar extension (cm year^{-1}) of colonies contained within the photoquadrats (0.5 × 0.5 m) recorded annually at 10 m depth on the fore reef at LTER 1. Colonies of *Pocillopora* spp. were haphazardly selected (regardless of size) in photoquadrats from any 1 year, and when they could be relocated in photoquadrats recorded 12 months later, their change in mean planar diameter was recorded. A variable number of colonies was tracked between each pair of years: growth rates for 2010 were based on 32 corals that were tracked from 2011 to 2012 (insufficient corals were present for scoring between 2010 and 2011), and for 2014, they were based on 278 colonies tracked from 2013 to 2014, and for 2017, they were based

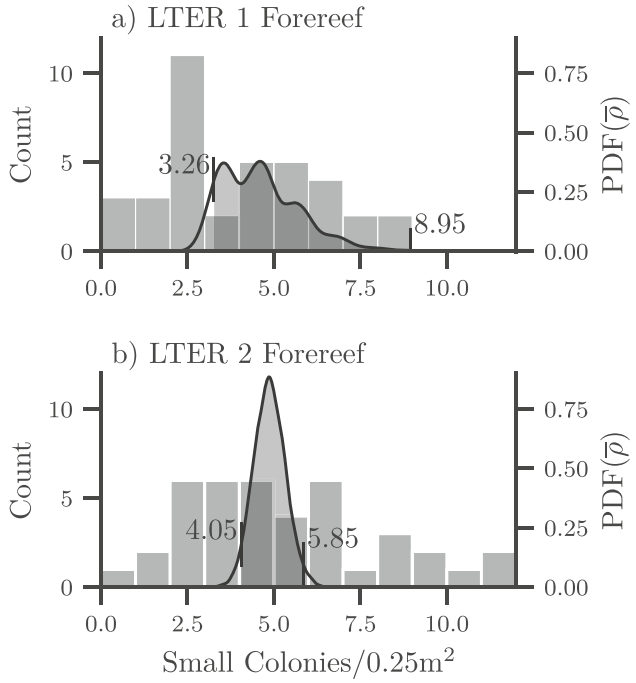

Fig. 5 **a**, **b** Histograms of small coral abundance per 0.25 m^2 quadrat for 2014 measured on the fore reef at sites LTER1 and LTER2. The right *y*-axis is a probability density function of the mean recruit flux as generated by 10^3 bootstrap samples. The 95% confidence interval bounds are labeled with ticks and shaded between. One measurement at LTER1 is not shown for clarity ($\rho = 45$) but is accounted for in the bootstrap resampling

on 10 colonies tracked from 2016 to 2017. Assuming the colonies of *Pocillopora* spp. were planar circles in outline, their growth rates were estimated as the change in diameter.

Mortality of *Pocillopora* spp. colonies

The annual mortality of *Pocillopora* spp. was quantified by tracking colonies recorded in photoquadrat (described above) between years at 10 m depth on the fore reef. Mortality for 2010 was estimated by tracking 61 colonies from 2011 to 2012 at LTER1 and LTER2; for 2014, it was estimated from 582 colonies tracked from 2013 to 2014 at LTER1 and LTER2; and for 2017, it was based on 62 colonies tracked from 2016 to 2017 at LTER1. Corals were scored as dead if not found in the subsequent year, thus providing annual mortality estimates of 26%, 27%, and 3%, respectively. Mortality data for *Pocillopora* spp. were not available for the back reef, but as a first approximation, we assumed mortality rates would be double those of the fore reef in any one year.

Pocillopora spp. fecundity (f)

Fecundity of *Pocillopora* spp. colonies was approximated from the number of eggs a colony might be expected to release in any 1 year and was expressed as eggs polyp^{-1} year^{-1}. Estimates of fecundity were found for *Pocillopora* spp. in the Maldives (7,300 eggs polyp^{-1} year^{-1} (Sier

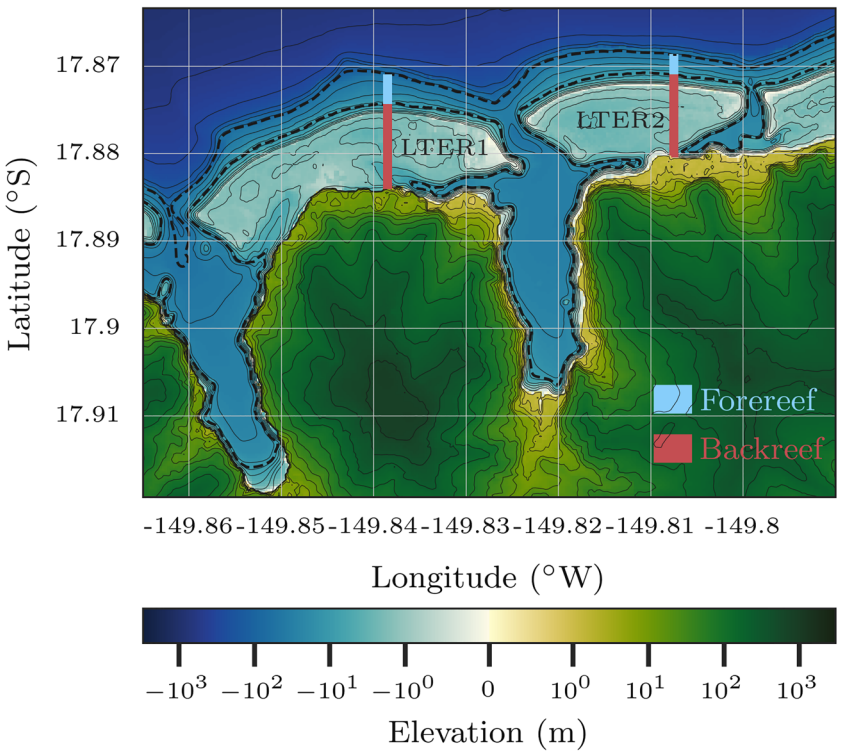

Fig. 6 A topographic map of a long-term study site on the north shore of Moorea, French Polynesia. 10-m and 60-m isobaths are indicated with black dashed contour lines. Color swaths are reef patches represented in the model and supported by field observations; each is divided into forereef (blue) and backreef (subpopulations)

and Olive 1994)), Hawai'i (7,524 eggs polyp^{-1} year^{-1} (Stimson 1976)), and the Red Sea (4158 eggs polyp^{-1} year^{-1} (Fadlallah 1985)). Mean fecundity was area-normalized using the polyp density of *Pocillopora* spp. in Hawaii (Tricas 1989), yielding a mean (± SE) fecundity of 95 ± 28 eggs polyp^{-1} year^{-1} (reported in Tsounis and Edmunds 2016).

Coral carrying capacity of *Pocillopora* spp. populations (K)

The carrying capacity (K) of the fore reef and back reef for *Pocillopora* spp. was estimated based on the maximum empirical coral cover (pooled among taxa) recorded, or as the total available hard substratum that might be colonized by corals. On the fore reef, the highest mean (± SE) coral cover at 10 m depth between 2011 and 2018 was recorded in 2018, with 80.9% at LTER1 and 64.7% at LTER2. For the back reef, K was estimated assuming all the planar area of hard substratum was filled by *Pocillopora* spp., with hard substratum in this habitat interspersed with sand.

Available hard substrata

The quantity (i.e., area) of hard substratum determines the maximum size of *Pocillopora* spp. populations in Moorea assuming it is all filled at the greatest empirical cover (on the forereef) or completely filled (back reef). The area of hard substratum at LTER1 and LTER2 was estimated from aerial images (accessed from Google Earth 24 August 2018) within a rectangle extending from the shore to the outer reef (long axis-oriented north–south). The rectangle was arbitrarily chosen to be 100 m wide, and within this width from the shore to the reef crest (71,609 m^2 at LTER1 and 70,600 m^2 at LTER2) areas of hard rock were measured by outlining in ImageJ software (Schneider et al. 2012). Available hard substrata occupied 45% of the back reef area at LTER1 and 49% of the area of the back reef at LTER2. The size of the available substratum on the fore reef was obtained by extending the same rectangles over the reef crest and estimating the planar area of the reef to the 10 m and the 60 m isobaths. The position of the isobaths was determined using bathymetric data compiled from an airborne LIDAR survey conducted in 2012 (Fugro LADS Corporation 2015) with shipboard multibeam echosoundings carried on the R/V Kilo Moana and R/V Ahi in 2013 (Fig. 6).

Supplementary Information The online version contains supplementary material available at https://doi.org/10.1007/s12080-024-00598-0.

Acknowledgements The field data were collected under permits issued by the French Polynesian Government (Délégation à la Recherche) and the Haut-Commissariat de la République en Polynésie-Française. With respect to the spelling of Moorea, we followed the Raapoto transcription system that is adhered to by a large segment of the Tahitian community, but also recognize other community members follow the Te Fare Vāna'a transcription system where the island name is spelled with an 'eta (Mo'orea).

Author contribution This paper is a product of an informal working group convened in 2018 that was led by Hollie Putnam and Jim Hench, funded through the Moorea Coral Reef Long Term Ecological Research Program, and in which all authors participated for 2–3 in-person meetings. All authors assisted in conceptualizing the model, but Walter Torres implemented the model as a formal construct and conducted the key analyses. Components of the model and data were contributed by all authors. Walter Torres wrote the first draft of the paper, and all authors participated in writing, reviewing, and editing. Dan Holstein, Rob Toonen, and Pete Edmunds contributed substantially to the discussion section. Jonathan Puritz, Dan Holstein, Walter Torres, and Jim Hench prepared the graphics. Hollie Putnam, and Jim Hench accessed and quality-controlled the ecological and physical observational data and wrote the appendix describing the data product.

Funding This work was supported by the U.S. National Science Foundation LTER program (OCE 2224354 and earlier awards) as well as a generous gift from the Gordon and Betty Moore Foundation. Additional support was provided by Duke University.

Data availability The online version provides and describes the data used in this manuscript. Python code for analysis and plotting with the accompanying data are available at https://doi.org/10.5281/zenodo.14232791.

Declarations

Conflict of interest The authors declare no competing interests.

References

Adjeroud M, Chancerelle C, Schrimm M, Perez T, Lecchini D, Galzin R, Salvat B (2005) Detecting the effects of natural disturbances on coral assemblages in French Polynesia: a decade survey at multiple scales. Aquat Living Resour 18:111–123. https://doi.org/10.1051/alr:2005014

Adjeroud M, Kayal M, Penin L (2017) Importance of recruitment processes in the dynamics and resilience of coral reef assemblages.

In: Rossi S (ed) Marine animal forests. Springer, Cham, pp 549–569 https://doi.org/10.1007/978-3-319-21012-4_12
Álvarez-Noriega M, Baird AH, Dornelas M, Madin JS, Cumbo VR, Connolly SR (2016) Fecundity and the demographic strategies of coral morphologies. Ecology 97(12):3485–3493. https://doi.org/10.1002/ecy.1588
Aronson R, Precht WF (1995) Landscape patterns of reef coral diversity: a test of the intermediate disturbance hypothesis. J Exp Mar Biol and Ecol 192:1–14. https://doi.org/10.1016/0022-0981(95)00052-S
Artzy-Randrup Y, Olinky R, Stone L (2007) Size-structured demographic models of coral populations. J Theor Biol 245(3):482–497. https://doi.org/10.1016/j.jtbi.2006.10.019
Baird AH, Guest JR, Willis BL (2009) Systematic and biogeographical patterns in the reproductive biology of scleractinian corals. Ann Rev Ecol Evol Syst 40:551–571. https://doi.org/10.1146/annurev.ecolsys.110308.120220
Beijbom O, Edmunds PJ, Roelfsema J, Smith DI, Kline BP, Neal MJ, Dunlap V, Moriarty TY, Fan CJ, Tan S, Chan T, Treibitz A, Gamst BG, Kriegman MD (2015) Towards automated annotation of benthic survey images: variability of human experts and operational modes of automation. PLOS ONE 10(7):e0130312. https://doi.org/10.1371/journal.pone.0130312
Burgess SC, Johnston EC, Wyatt ASJ, Leichter JJ, Edmunds PJ (2021) Response diversity in corals: hidden differences in bleaching mortality among cryptic Pocillopora species. Ecology 102(6):e03324. https://doi.org/10.1002/ecy.3324
Carroll A, Harrison P, Adjeroud M (2006) Sexual reproduction of Acropora reef corals at Mo'orea, French Polynesia. Coral Reefs 25:93–97. https://doi.org/10.1007/s00338-005-0057-6
Darling ES, Côté, IM (2018) Seeking resilience in marine ecosystems. Science 359:986–987, https://doi.org/10.1126/science.aas9852
Dietzel A, Bode M, Connolly SR, Hughes TP (2021) The population sizes and global extinction risk of reef-building coral species at biogeographic scales. Nat Ecol Evol 5:663–669. https://doi.org/10.1038/s41559-021-01393-4
Edmunds PJ, Leichter JJ, Adjeroud M (2010) Landscape-scale variation in coral recruitment in Moorea, French Polynesia. Mar Ecol Prog Ser 414:75–89. https://doi.org/10.3354/meps08728
Edmunds PJ, McIlroy SE, Adjeroud M, Ang P, Bergman JL, Carpenter RC, Coffroth MA, Fujimura AG, Hench JL, Holbrook SJ, Leichter JJ, Muko S, Nakajima Y, Nakamura M, Paris CB, Schmitt RJ, Sutthacheap M, Toonen RJ, Sakai K, Suzuki G, Washburn L, Wyatt ASJ, Mitarai S (2018) Critical information gaps impeding understanding of the role of larval connectivity among coral reef islands in an era of global change. Front Mar Sci 5:1–16. https://doi.org/10.3389/fmars.2018.00290
Edmunds PJ, Maritorena S, Burgess SC (2024) Early post-settlement events, rather than settlement, drive recruitment and coral recovery at Moorea, French Polynesia. Oecologia 204:625–640
Fadlallah Y (1985) Reproduction in the coral Pocillopora verrucosa on the reefs adjacent to the industrial city of Yanbu (Red Sea, Saudi Arabia). In: Proc 5th Int Coral Reef Conf, Vol 4, pp 313–318
Figueira WF (2009) Connectivity or demography: defining sources and sinks in coral reef fish metapopulations. Ecol Modell 220:1126–1137. https://doi.org/10.1016/j.ecolmodel.2009.01.021
Fugro LADS Corporation (2015). Airborne LIDAR bathymetric survey of French Polynesia 2015, Document number TLCS00.046.009, Prepared for J.L. Hench (PI), 186 pages.
Garavelli L, White JW, Chollett I, Cherubin L (2018) Population models reveal unexpected patterns of local persistence despite widespread larval dispersal in a highly exploited species. Conserv Lett 11:e12567. https://doi.org/10.1111/conl.12567
Hall VR, Hughes TP (1996) Reproductive strategies of modular organisms: comparative studies of reef-building corals. Ecology 77(3):950–963. https://doi.org/10.2307/2265514
Han X, Adam TC, Schmitt RJ, Brooks AJ, Holbrook SJ (2016) Response of herbivore functional groups to sequential perturbations in Moorea, French Polynesia. Coral Reefs 35:997–1007. https://doi.org/10.1007/s00338-016-1423-2
Hanski I, Ovaskainen O (2000) The metapopulation capacity of a fragmented landscape. Nature 404:755–758. https://doi.org/10.1038/35008063
Hastings A, Botsford LW (2006) Persistence of spatial populations depends on returning home. Proc Natl Acad Sci 103(15):6067–6072. https://doi.org/10.1073/pnas.0506651103
Hench JL, Leichter JJ, Monismith SG (2008) Episodic circulation and exchange in a wave-driven coral reef and lagoon system. Limnol Oceanogr 53:2681–2694. https://doi.org/10.4319/lo.2008.53.6.2681
Hoegh-Guldberg O, Mumby PJ, Hooten AJ, Steneck RS, Greenfield P, Gomez E, Harvell CD, Sale PF, Edwards AJ, Caldeira K, Knowlton N, Eakin CM, Iglesias-Prieto R, Muthiga N, Bradbury RH, Dubi A, Hatziolos ME (2011) Coral reefs under rapid climate change and ocean acidification. Science 318(5857):1737–1742. https://doi.org/10.1126/science.1152509
Holbrook SJ, Adam TC, Edmunds PJ, Schmitt RJ, Carpenter RC, Brooks AJ, Lenihan HS, Briggs CJ (2018) Recruitment drives spatial variation in recovery rates of resilient coral reefs. Sci Rep 8:7338. https://doi.org/10.1038/s41598-018-25414-8
Holstein DM, Smith TB, Gyory J, Paris CB (2015) Fertile fathoms: deep reproductive refugia for threatened shallow corals. Sci Rep 5:12407. https://doi.org/10.1038/srep12407
Holstein DM, Smith TB, van Hooidonk R, Paris CB (2022) Predicting coral metapopulation decline in a changing thermal environment. Coral Reefs 41:961–972
Hughes TP (1984) Population dynamics based on size or age? a reef-coral analysis. Am Nat 129(6):818–829. https://doi.org/10.1086/284677
Hughes TP (1994) Catastrophes, phase shifts, and large-scale degradation of a Caribbean coral reef. Science 265(5178):1547–1551. https://doi.org/10.1126/science.265.5178.1547
Husniah H, Supriatna AK (2014) Marine biological metapopulation with coupled logistic growth functions: the MSY and quasi MSY. AIP Conf Proc 1587(1):51–56. https://doi.org/10.1063/1.4866532
Kaya M, Lenihan HS, Brooks AJ, Holbrook SJ, Schmitt RJ, Kendall BE (2018) Predicting coral community recovery using multispecies population dynamics models. Ecol Lett 21:1790–1799. https://doi.org/10.1111/ele.13153
Lindhart M (2022) Loss of reef roughness increases residence time on an idealized coral reef. Sci Rep 12:19410. https://doi.org/10.1038/s41598-022-24045-4
Magalon H, Adjeroud M, Veuille M (2005) Patterns of genetic variation do not correlate with geographical distance in the reef-building coral Pocillopora meandrina in the South Pacific. Mol Ecol 14:1861–1868. https://doi.org/10.1111/j.1365-294X,2004.02430.x
Merow C, Dahlgren JP, Metcalf CJE, Childs DZ, Evans ME, Jongejans E, Record S, Rees M, Salguero-Gomez R, McMahon SM (2014) Advancing population ecology with integral projection models: a practical guide. Methods Ecol Evol 5:99–110. https://doi.org/10.1111/2041-210X.12146
Mitarai S, Siegel DA, Watson JR, Dong C, McWilliams JC (2009) Quantifying connectivity in the coastal ocean with application to the Southern California Bight. J Geophys Res (Oceans) 114(C10):C10026. https://doi.org/10.1029/2008JC005166
Moeller HV, Neubert MG (2015) Economically optimal marine reserves without spatial heterogeneity in a simple two-patch model. Nat Resour Model 28(3):244–255. https://doi.org/10.1111/nrm.12066
Monismith SG, Herdman LMM, Ahmerkamp SH, Hench JL (2013) Wave transformation and wave-driven flow across a steep coral reef. J Phys Oceanogr 43:1356–1379. https://doi.org/10.1175/JPO-D-12-0164.1

Mumby P, Foster N, Fahy E (2005) Patch dynamics of coral reef macroalgae under chronic and acute disturbance. Coral Reefs 24:681–692. https://doi.org/10.1007/s00338-005-0058-5

Osborne K, Dolman AM, Burgess SC, Johns KA (2011) Disturbance and the dynamics of coral cover on the great barrier reef (1995–2009). PLoS ONE 6(3):e17516. https://doi.org/10.1371/journal.pone.0017516

Padilla-Gamiño JL, Gates DR (2012) Spawning dynamics in the Hawaiian reef-building coral Montipora capitata. Mar Ecol Prog Ser 449:145–160. https://doi.org/10.3354/meps09530

Pulliam HR, Danielson BJ (1991) Sources, sinks, and habitat selection: a landscape perspective on population dynamics. Am Nat 137:S50–S66. https://doi.org/10.1086/285139

Quigley KM, Bay LK, van Oppen MJH (2019) The active spread of adaptive variation for reef resilience. Ecol Evol 9:11122–11135. https://doi.org/10.1002/ece3.5616

Reverter M, Jackson M, Rohde S, Moeller M, Bara R, Lasut MT, Reinach MS, Schupp PJ (2022) High taxonomic resolution surveys and trait-based analyses reveal multiple benthic regimes in North Sulawesi (Indonesia). Sci Rep 11:16554. https://doi.org/10.1038/s41598-021-95905-81

Rinkevich B, Loya Y (1986) Senescence and dying signals in a reef building coral. Experientia 42:320–322. https://doi.org/10.1007/BF01942521

Scheltema RS (1986) Long-distance dispersal by planktonic larvae of shoal-water benthic invertebrates among central Pacific islands. Bull Mar Sci 39:241–256

Schmitt RJ, Holbrook SJ, Davis SL, Adam TC (2019) Experimental support for alternative attractors on coral reefs. Proc Natl Acad Sci 116:4372–4381. https://doi.org/10.1073/pnas.1812412116

Schneider CA, Rasband WS, Eliceiri KW (2012) NIH Image to ImageJ: 25 years of image analysis. Nat Methods 9(7):671–675. https://doi.org/10.1038/nmeth.2089

Sier CJS, Olive PJW (1994) Reproduction and reproductive variability in the coral Pocillopora verrucosa from the Republic of Maldives. Mar Biol 118:713–722. https://doi.org/10.1007/BF00347520

Stimson JS (1976) Reproduction of some common Hawaiian reef corals. In: Mackie GO (ed) Coelenterate ecology and behavior. Springer, New York, pp 271–279

Syms C, Jones GP, Symsi C (2000) Disturbance, habitat structure, and the dynamics of a coral-reef fish community. Ecology 81:2714–2729. https://doi.org/10.2307/177336

Tricas TC (1989) Determinants of feeding territory size in the corallivorous butterflyfish, Chaetodon mufticinctus. Anim Behav 37:830–841. https://doi.org/10.1016/0003-3472(89)90067-5

Tsounis G, Edmunds PJ (2016) The potential for self-seeding by the coral Pocillopora spp. in Moorea. French Polynesia. Peerj 4:e2544. https://doi.org/10.7717/peerj.2544

Vercelloni J, Kayal M, Chancerelle Y, Planes S (2019) Exposure, vulnerability, and resiliency of French Polynesian coral reefs to environmental disturbances. Sci Rep 9:1027. https://doi.org/10.1038/s41598-018-38228-5

Verhulst PF (1845) Recherches mathématiques sur la loi d'accroissement de la population. Nouv. m´em. de l'Academie Royale des Sci. et Belles-Lettres de Bruxelles 18:1–41

Vermeij MJ, Sandin SA (2008) Density-dependent settlement and mortality structure the earliest life phases of a coral population. Ecology 89:1994–2004. https://doi.org/10.1890/07-1296.1

Virtanen P, Gommers R, Oliphant TE, Haberland M, Reddy T, Cournapeau D, Burovski E, Peterson P, Weckesser W, Bright J, van der Walt SJ, Brett M, Wilson J, Millman KJ, Mayorov N, Nelson ARJ, Jones E, Kern R, Larson E, Carey CJ, Polat I, Feng Y, Moore EW, VanderPlas J, Laxalde D, Perktold J, Cimrman R, Henriksen I, Quintero EA, Harris CR, Archibald AM, Ribeiro AH, Pedregosa F, van Mulbregt P, SciPy 1.0 Contributors (2020) SciPy 1.0: fundamental algorithms for scientific computing in python. Nat Methods 17:261–272. https://doi.org/10.1038/s41592-019-0686-2